



# Application of Doehlert experimental design for the removal of radium from aqueous solution by cross-linked phenoxycalix[4]pyrrole-polymer using Ba(II) as a model

Nancy AlHaddad<sup>1,2</sup> · Radwan Sidaoui<sup>1</sup> · Malek Tabbal<sup>3</sup> · Ismail Abbas<sup>4</sup> · Pierre-Edouard Danjou<sup>2</sup> · Francine Cazier-Dennin<sup>2</sup> · Rana Baydoun<sup>1</sup> · Omar EL Samad<sup>1</sup> · Ahmad Rifai<sup>1</sup>

Received: 12 July 2019 / Accepted: 11 November 2019 / Published online: 12 December 2019  
© Springer-Verlag GmbH Germany, part of Springer Nature 2019

## Abstract

Ra-226 is a naturally occurring radionuclide that is derived from uranium-238 series, and it is present at low concentrations in rocks, soil, and groundwater. Many efforts have been exerted for the decontamination of radium from aqueous media in order to meet the increasing water demand of the population. To this aim, a new polymer based on cross-linked phenoxycalix[4]pyrrole was designed and employed in solid/liquid extractions in order to remove radium from aqueous solutions. Preliminary experiments have highlighted the capability of this polymer to extract 22% of Ra-226 from aqueous acidic solution. The optimization of the extraction experimental factors in the direction to attend the maximum removal of Ra-226 from water was carried out employing Ba<sup>2+</sup> due to its similar chemical behavior as radium, in order to minimize the consumption of Ra-226 solutions and the risk of radioactive contamination. Doehlert experimental plan was then applied to determine the optimal conditions (pH, time, temperature) for the removal of Ba<sup>2+</sup> from aqueous solutions.

**Keywords** Calix[4]pyrrole polymer · Ra-226 removal · Doehlert system · Optimal conditions of extraction

## Introduction

Increasing urbanization and industrialization, the rise in population and associated increased water demands have placed

tremendous pressure on available water resources, accelerating thus the rates of their depletion and contamination. Subsequent environmental damage and pollution of aquatic environments by several organic and inorganic contaminants became a major and constant threat to the water resources and all the living beings. For that, emerging interests and efforts are devoted nowadays to develop new techniques capable of extracting these contaminants from aqueous solutions. Methods like precipitation, liquid-liquid extraction, membrane filtration, and ion exchange are usually considered classic and, so far, engaged the most in the process of water decontamination.

Radium is one of the most radiotoxic inorganic metals present in the environment (Eisenbud and Gesell 1997; Matyskin et al. 2019). This element belongs to alkaline-earth metals of the second periodic table group. It is found in uranium and to a lesser extent in thorium ores in trace amounts. Its main radioisotopes are Ra-228 and Ra-224 occurring naturally in the decay chain of Th-232; and Ra-226 and Ra-223 occurring in U-238 and U-235 decay chains respectively. Ra-226 is the focus of our study; it is an alpha emitter with long half-life ( $T_{1/2} = 1602$  years), which increased the concerns from the viewpoint of health risks (Zielinski et al. 2011). It emits

---

Responsible editor: Philippe Garrigues

**Electronic supplementary material** The online version of this article (<https://doi.org/10.1007/s11356-019-07021-w>) contains supplementary material, which is available to authorized users.

✉ Ahmad Rifai  
ahmad.rifaii@cnrs.edu.lb

<sup>1</sup> Lebanese Atomic Energy Commission, National Council for Scientific Research, B.P.11-8281, Riad El Solh1107, Beirut 2260, Lebanon

<sup>2</sup> Unité de Chimie Environnementale et Interactions sur le Vivant (UCEIV), Université du Littoral Côte d'Opale, 145 Avenue Maurice Schumann, MREI 1, 59140 Dunkerque, France

<sup>3</sup> Central Research Science Laboratory, Physics Building, American University of Beirut, P.O.Box 11-0236, Physics Dept. Riad El-Solh, Beirut 1107 2020, Lebanon

<sup>4</sup> Faculty of Sciences, Lebanese University, Mount of Lebanon, Hadath, Lebanon

gamma radiation at 186.2 keV. It is found naturally in soil, rocks (Sharma et al. 2019; Majeed et al. 2019), groundwater (Vengosh et al. 2009; Zielinski et al. 2011; Yang et al. 2018), and minerals that contain radionuclides. Its concentration in the environment could be increased due to anthropic industrial activities such as uranium mining, oil and gas production, and phosphate fertilizer production (Ward Whicker 1997; Bassioni et al. 2012; McDevitt et al. 2018).

Many countries were interested in the removal of Ra-226 from aqueous media, and various techniques were developed for this purpose such as precipitation, extraction, ion exchange, or complexation (Mishra and Tiwary 1999; McDowell et al. 1986; Vengosh et al. 2009; Kondash et al. 2013; Zhang et al. 2014; Fard et al. 2016; Mokhodoeva et al. 2016; Nafae et al. 2016; Zayir et al. 2016; Gott et al. 2019; Reissig et al. 2019). Organic compounds like calixarenes and crown ethers macromolecules have been used as complexing platforms for removal of several stable and radioactive alkaline-earth elements from aqueous media (Chen et al. 1999; Chirarizia et al. 1999; Henriksena et al. 2002). To the best of our knowledge, there is no literature dedicated to the use of phenoxy-calix[4]pyrrole polymers for the removal of environmentally relevant species like heavy metals or radionuclides. Originally described in 1999 by Sessler (Anzenbacher et al. 1999) and Floriani (Bonomo et al. 1999) groups,  $\alpha\alpha\alpha\alpha$ -phenoxy-calix[4]pyrrole (Scheme 1) was firstly studied for its anion chelation properties (Camiolo and Gale 2000). Nevertheless, the presence of four easily functionalizable phenoxy groups oriented in the same direction has inspired our group (Danil de Namor et al. 2007a, b; Abbass and Chaaban 2012; Rifai et al. 2019) and others (Danil de Namor and Khalife 2008; Chi et al. 2017) to use the chelate effect to recognize cations. In this work, epichlorohydrin was employed to crosslink the pre-organized supramolecular platform (i.e., phenoxy-calix[4]pyrrole) while introducing numerous ether bridges dedicated to cationic species chelation. The water-insoluble polymer (CPP) thus obtained was subjected to preliminary tests to determine its capacity to remove Ra-226 from aqueous solutions via solid/liquid extractions and gave encouraging results of 22% extraction efficiency. Noting that the removal of any material (organic or inorganic) from aqueous media using solid/liquid extractions could be affected by several experimental factors as pH, temperature, and time, a statistical plan was applied to identify the optimal experimental conditions of extraction (Abbas et al. 2012) to optimize the removal efficiency of Ra-226 by the newly developed polymer. In order to minimize the consumption of radioactive Ra-226 solutions and the risk of radioactive contamination,  $Ba^{2+}$  was used as model during extraction experiments due to its similar chemical behavior as radium (alkaline-earth metals).

The traditional and conventional technique used for the optimization is the “one factor at a time,” in which a single

parameter is varied while other factors are fixed at a specific level. It ignores the interaction among the process variables and might lead to unreliable results as it requires a large number of experiments. These drawbacks of single parameter optimization process are improved by considering several affecting parameters collectively via Doehlert experimental design of response surface methodology (RSM) (Doehlert 1970). The optimization based on RSM involves three major steps of (a) conducting a statistically designed experiment, (b) fitting experimental data within a quadratic model and determining the corresponding coefficients, and (c) predicting the response and checking the adequacy of the model (Vanot et al. 2002; Ferreira et al. 2004; Dutra et al. 2006; Imandi et al. 2007; Karanam and Medicherla 2010; Silas et al. 2016). In this study, a customized Doehlert experimental design of response surface methodology (RSM) was applied to evaluate the application potential of CPP for the decontamination of radium from aqueous media through the study of its extraction behavior towards  $Ba^{2+}$ .

## Materials and methods

### Phenoxy-calix[4]pyrrole polymer synthesis

Phenoxy-calix[4]pyrrole polymer (CPP) was synthesized in water from  $\alpha\alpha\alpha\alpha$ -phenoxy-calix[4]pyrrole and epichlorohydrin according to the procedure described by Danjou et al. (AlHaddad et al., 2019). Briefly, phenoxy-calix[4]pyrrole (1.0 g) was dissolved in NaOH aqueous solution (16 equiv., 20 mL) for 30 min. Then, epichlorohydrin (32 equiv.) was added and the resulting mixture was stirred at 80 °C during 4 h. Solid CPP was recovered by filtration and washed thoroughly with ultrapure water to afford a light brown powder.

### Preliminary extraction test of CPP for Ra-226 removal

In order to test the efficiency of CPP for Ra-226 removal, 300 mg of CPP was added to 100 mL solution of Ra-226 having an activity concentration of  $81 \pm 5 \text{ Bq kg}^{-1}$ , prepared from the digestion of a soil leftover proficiency test sample IAEA-CU-2010-03. The extraction process was carried out at room temperature, pH = 2 and a contact time of 5 min. Measurements before and after extraction were carried out using a gamma spectrometer with high-purity germanium detector.

### Experimental conditions for the effect of CPP dose

Barium perchlorate stock solution (3000 mg/L) in deionized water (stored at 4 °C) has been used as a reference solution. Working solutions (50 mg/L) have been prepared and used during extraction experiments. The effect of CPP dose on

the efficiency of extraction has been studied by adding incremented quantities of CPP (5 to 300 mg) to 20 mL solutions containing 50 mg/L of Ba<sup>2+</sup> solutions at pH 6.5. The solutions were shaken in a thermostated water bath at 25 °C. After 15 min, the solutions were centrifuged and the concentrations of Ba<sup>2+</sup> ions remaining in the solutions were determined by flame atomic absorption spectroscopy (AAS) using barium primary wavelength at 553.6 nm.

**Experimental conditions for effects of pH, contact time, and temperature**

A set of working solutions at 50 mg/L of Ba<sup>2+</sup> has been prepared at different pH values (3, 4.5, 6, 7.5, and 9) from the same stock solution using nitric acid (1N) or sodium hydroxide (1N) for pH adjustment. These solutions were divided into 20 mL in centrifuging tubes and 75 mg of CPP was added for each for the solid/liquid extractions. Tubes were placed in thermostated water bath for different time intervals (5, 25, 40, 55, 70, 85, and 100 min) at different temperatures (25, 35, and 45 °C) as shown in Table 1. Solid/liquid separation has been done by centrifugation (3000 rpm for 5 min) and the concentrations of Ba<sup>2+</sup> ions remaining in solutions were determined by AAS. These experiments were repeated twice.

The removal percentage of Ba<sup>2+</sup> by CPP from the tested aqueous solutions is given by the following equation:

$$\% \text{ removal} = \frac{(C_0 - C_i)}{C_0} \times 100 \tag{1}$$

where C<sub>0</sub> is the initial concentration of Ba<sup>2+</sup> and C<sub>i</sub> is the final concentration upon extraction.

**Doehlert experimental design**

A Doehlert experimental plan was conducted on 15 experimental runs in triplicate by taking into consideration 3 parameters: pH, contact time, and temperature. This plan requires a limited number of planned experiments that involve

interaction of process variables and allows the modeling of the obtained experimental data by Eq. 2:

$$Y_{\text{response}} = f(X, \beta) \text{ (model)} + \varepsilon \text{ (error)} \tag{2}$$

where f(X, β) represents the response surface and ε the random experimental that is assumed to follow a normal probability distribution with constant experimental variance.

The second degree polynomial (Eq. 3) was fitted to the experimental data, using the statistical package STATISTICA 7 in order to estimate the response of the dependent variable and the regression coefficients (β). These unknown coefficients are estimated by multiple regression and the response surface is given by Eq. 3:

$$Y = \beta_0 + \beta_1 X_1 + \beta_2 X_2 + \beta_3 X_3 + \beta_{12} X_1 X_2 + \beta_{13} X_1 X_3 + \beta_{23} X_2 X_3 + \beta_{11} X_1^2 + \beta_{22} X_2^2 + \beta_{33} X_3^2 + \varepsilon \tag{3}$$

where Y is the measured response; X<sub>1</sub>, X<sub>2</sub>, and X<sub>3</sub> are independent variables; β<sub>1</sub>, β<sub>2</sub>, and β<sub>3</sub> are the coefficients for linear effects; β<sub>12</sub>, β<sub>13</sub>, and β<sub>23</sub> are the coefficients for interaction terms; and β<sub>11</sub>, β<sub>22</sub>, and β<sub>33</sub> are the coefficients for squared effects (Karanam and Medicherla 2010).

In order to calculate the coordinates of the optimal conditions X<sub>s</sub> (represented by X<sub>1s</sub>, X<sub>2s</sub>, X<sub>3s</sub>), it is necessary to determine the derivatives of Eq. 3 with respect to the three independent variables after equating them to zero. These derivative equations are presented by Eq. 4:

$$\begin{aligned} \frac{\partial Y}{\partial X_1} &= \beta_1 + \beta_{12} X_2 + \beta_{13} X_3 + 2\beta_{11} X_1 = 0 \\ \frac{\partial Y}{\partial X_2} &= \beta_2 + \beta_{12} X_1 + \beta_{23} X_3 + 2\beta_{22} X_2 = 0 \\ \frac{\partial Y}{\partial X_3} &= \beta_3 + \beta_{13} X_1 + \beta_{23} X_2 + 2\beta_{33} X_3 = 0 \end{aligned} \tag{4}$$

Later, a matrix B was introduced in order to identify X<sub>s</sub>. It can be represented by any of the following situations that

**Table 1** Experimental range and levels of the considered factors

Variables	Range and levels							
Coded variable1 (x1)	-1	-0.5	0	0.5	1			
pH(X1)	3	4.5	6	7.5	9			
Coded variable2 (x2)	$\frac{-\sqrt{3}}{2}$	$\frac{-\sqrt{3}}{3}$	$\frac{-\sqrt{3}}{6}$	0	$\frac{\sqrt{3}}{6}$	$\frac{\sqrt{3}}{3}$	$\frac{\sqrt{3}}{2}$	
Time(X2)	10	25	40	55	70	85	100	
Coded variable3 (x3)	$\frac{-\sqrt{6}}{3}$	0	$\frac{\sqrt{6}}{3}$					
Temperature (X3)	25	35	45					

depend on the sign of eigenvalues (EV): Accordingly, in respective to all EV, whether they are positive or negative, the response surface will be minimal or maximal. The matrix **B** is presented by:

$$B = \begin{vmatrix} 2\beta_{11} & \beta_{12} & \beta_{13} \\ \beta_{12} & 2\beta_{22} & \beta_{23} \\ \beta_{13} & \beta_{23} & 2\beta_{33} \end{vmatrix}$$

**B** is a (3×3) symmetric matrix which main diagonal elements are the pure quadratic coefficients ( $\beta_{ii}$ ), and the other elements occupying, in a symmetrical way, the other zones of the matrix consist of interaction coefficients ( $\beta_{ij}$ ) with  $\beta_{ij} = \beta_{ji}$ .

The inverse of matrix **B** multiplication by the negative values of the main coefficients of linear effects ( $\beta_L$ ) gives the optimal value of every factor (critical values:  $X_{1s}$ ,  $X_{2s}$ ,  $X_{3s}$ ). The derivative equation and the general matrix for  $X_s$  are presented by the Eqs. 4 and 5:

$$\frac{\delta Y}{\delta X} = \beta_L + B * X_s = 0 \quad (5)$$

$$X_s = \begin{vmatrix} X_{1s} \\ X_{2s} \\ X_{3s} \end{vmatrix} = \begin{vmatrix} 2\beta_{11} & \beta_{12} & \beta_{13} \\ \beta_{12} & 2\beta_{22} & \beta_{23} \\ \beta_{13} & \beta_{23} & 2\beta_{33} \end{vmatrix}^{-1} \begin{vmatrix} -\beta_1 \\ -\beta_2 \\ -\beta_3 \end{vmatrix}$$

In the present study, the conditions with the coded variables have been presented in Table 1

## Results and discussions

### Preliminary extraction test of CPP for Ra-226 removal

A preliminary solid/liquid extraction of Ra-226 by **CCP** was conducted under non-optimized conditions on a real aqueous sample containing Ra-226 whose activity has been measured at  $81 \pm 5$  Bq kg<sup>-1</sup>. After a few minutes of contact with **CPP**, the polymer was removed and the activity of the remaining solution was measured at  $63 \pm 4$  Bq kg<sup>-1</sup>. In view of this promising result, it was decided to optimize the parameters influencing the extraction of Ra-226 by **CPP** using Ba<sup>2+</sup> as a model to avoid radioactive waste.

### Effect of CPP dose

**CPP** is completely insoluble in water and as such, it could be used in solid/liquid extraction of pollutants (stable or radioactive) from aqueous media. As demonstrated in Fig. 1, the effect of **CPP** quantity on the removal of Ba<sup>2+</sup> ions from aqueous media was investigated. This study was done by varying the amount of the polymer while keeping other

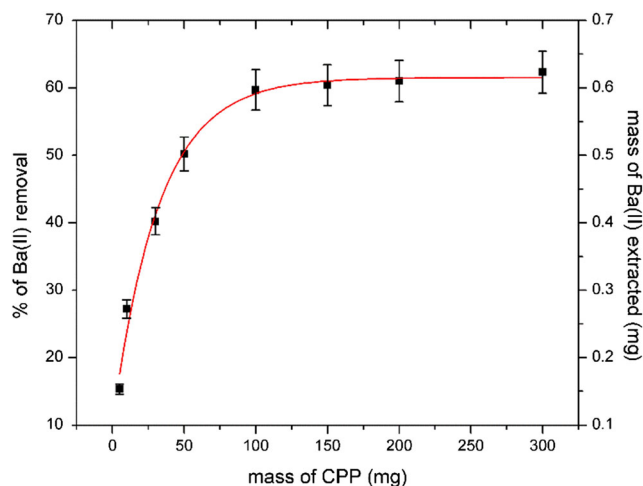


**Fig. 1** The effect of CPPs' amount on the removal of barium in terms of percentage and extracted mass

conditions (pH, temperature, contact time, and the concentration of Ba<sup>2+</sup> (50 ppm)) constant. It is obvious that the amount of Ba<sup>2+</sup> ions removed from solution increases as the mass of the polymer increases for a given initial concentration. This may be attributed to the presence of more binding sites for interaction with Ba<sup>2+</sup> ions. The highest quantity of Ba<sup>2+</sup> was extracted by using 75 mg of the polymer and allowed to estimate the maximal sorption capacity of Ba<sup>2+</sup> by **CPP** at 8 mg/g. In fact, upon use of quantities larger than 75 mg, no significant changes were detected for the percentage of extraction. So, 75 mg of **CPP** was selected as optimum for further extraction experiments.

### Optimization of experimental conditions using Doehlert design

In order to evaluate the extraction capacities of **CCP** towards Ba<sup>2+</sup>, it is essential to consider the optimization of 3 variables (pH, contact time, and temperature) that could affect and increase the efficiency for the removal of contaminants from aqueous media. In an effort to avoid the broad number of experiments used in “one factor fixed at a time” techniques, Doehlert experimental plan appeared to be a valuable solution to achieve our aim. The selection for the range of process variables is significant when planning the experimental design. Otherwise, after experiment completion, the optimal conditions obtained by response surface methodology might not be found inside the experimental region. Fifteen experimental runs including three replicates at the center points were carried out. In order to compare the effect of the three factors on the removal of Ba<sup>2+</sup>, two experimental plans have been placed. The first one, named “system 1” is the same method used by Silas et al. and has been coded by **S1** ( $X_1$ ,  $X_2$ ,  $X_3$ ) where  $X_1$  are

**Table 2** Experimental and predicted values of the three factors ( $X_1$ ,  $X_2$ , and  $X_3$ ) for S1 according to Doehlert experimental design

No.	Coded values			Natural values			% of barium extraction	
	$x_1$	$x_2$	$x_3$	pH ( $X_1$ )	Time of contact ( $X_2$ )	Temperature ( $X_3$ )	Observed	Predicted
1	-1/2	$\sqrt{3}/2$	0	4.5	100	35	74.06	64.01
2	1/2	$\sqrt{3}/2$	0	7.5	100	35	26.27	35.06
3	0	$\sqrt{3}/3$	$-\sqrt{6}/3$	6	85	25	73.37	74.63
4	-1/2	$\sqrt{3}/6$	$\sqrt{6}/3$	4.5	70	45	68.94	63.09
5	1/2	$\sqrt{3}/6$	$\sqrt{6}/3$	7.5	70	45	26.79	33.89
6	-1	0	0	3	55	35	40.61	56.50
7	0	0	0	6	55	35	76.62	75.65
8	1	0	0	9	55	35	13.31	12.58
9	-1/2	$-\sqrt{3}/6$	$-\sqrt{6}/3$	4.5	40	25	72.86	65.76
10	1/2	$-\sqrt{3}/6$	$-\sqrt{6}/3$	7.5	40	25	30.03	35.87
11	0	$-\sqrt{3}/3$	$\sqrt{6}/3$	6	25	45	71.67	70.41
12	-1/2	$-\sqrt{3}/2$	0	4.5	10	35	71.50	62.71
13	1/2	$-\sqrt{3}/2$	0	7.5	10	35	22.52	32.57
14	0	0	0	6	55	35	76.45	75.65
15	0	0	0	6	55	35	73.89	75.65

the values of pH,  $X_2$  the values of contact time, and  $X_3$  the values of temperature. The second system named “system 2,” has been designed through changing the maximum values of  $X_3$  by the minimum ones and by keeping the same values for the center; this system has been coded by S2 ( $X_1$ ,  $X_2$ ,  $-X_3$ ). All data for S1 and S2 including the coded values, the natural values of the three factors, as well as experimental and predicted values for the removal

percentage of  $Ba^{2+}$  have been represented in Tables 2 and 3.

Using MATLAB (regstats) and STATISTICA 7 programs,  $Y$  functions of Eq. 3 were estimated for S1 and S2 and are presented below:

**S 1**

$$Y = - 227.9 + 54.6652X_1 + 2.0211X_2 + 6.6017X_3 + 0.0044X_1X_2 + 0.0047X_1X_3 - 0.0348X_2X_3 - 5.4102X_1^2 - 0.0074X_2^2 - 0.0695X_3^2$$

**Table 3** Experimental and predicted values of the three factors ( $X_1$ ,  $X_2$ , and  $-X_3$ ) for S2 according to Doehlert experimental design

No.	Coded values			Natural values			% of barium extraction	
	$x_1$	$x_2$	$x_3$	pH ( $X_1$ )	Time of contact ( $X_2$ )	Temperature ( $X_3$ )	Observed	Predicted
1	-1/2	$\sqrt{3}/2$	0	4.5	100	35	74.06	64.01
2	1/2	$\sqrt{3}/2$	0	7.5	100	35	26.27	34.44
3	0	$\sqrt{3}/3$	$\sqrt{6}/3$	6	85	45	74.23	76.08
4	-1/2	$\sqrt{3}/6$	$-\sqrt{6}/3$	4.5	70	25	72.69	66.19
5	1/2	$\sqrt{3}/6$	$-\sqrt{6}/3$	7.5	70	25	23.37	31.74
6	-1	0	0	3	55	35	40.61	57.14
7	0	0	0	6	55	35	76.62	75.65
8	1	0	0	9	55	35	13.31	13.22
9	-1/2	$-\sqrt{3}/6$	$\sqrt{6}/3$	4.5	40	45	72.86	64.50
10	1/2	$-\sqrt{3}/6$	$\sqrt{6}/3$	7.5	40	45	32.08	38.58
11	0	$-\sqrt{3}/3$	$-\sqrt{6}/3$	6	25	25	74.06	72.20
12	-1/2	$-\sqrt{3}/2$	0	4.5	10	35	71.50	63.33
13	1/2	$-\sqrt{3}/2$	0	7.5	10	35	22.52	32.55
14	0	0	0	6	55	35	76.45	75.65
15	0	0	0	6	55	35	73.89	75.65

**S 2**

$$Y = - 56.6143 + 49.4083X_1 - 0.5007X_2 + 1.4263X_3 + 0.0044X_1X_2 + 0.1488X_1X_3 + 0.0371X_2X_3 - 5.4102X_1^2 - 0.0074X_2^2 - 0.0601 X_3^2$$

The confidence interval explains how the variation could be possible with a certain model. The uncertainty in the specific estimate is reflected by prediction interval, and logically the error is greater than the confidence interval. Unlike confidence interval, prediction interval predicts the spread for “individual” observation, rather than the mean value (Silas et al. 2016). As shown in Fig. 2, the distribution of the fitting parameters is very similar and shows a satisfactory correlation between the predicted and the observed data with an acceptable uncertainty for systems 1 and 2. The predicted percentages for removal of Ba<sup>2+</sup> from solutions presented by solving Eq. 3 are in good agreement with the experimental results presented in Table 4 and Fig. 2. Subsequently, the above equation was considered as appropriate to find the percentage of removal of Ba<sup>2+</sup> from aqueous media under the specific range of experiments.

It is possible to calculate the coordinates of the optimal conditions through the response of surface and equate them to zero. The equations for the three variables for S1 and S2 are presented below (Eq. 4):

**S 1**

$$\begin{aligned} \frac{\partial Y}{\partial X_1} &= 54.6652 + 0.0044 X_2 + 0.0047X_3 - 10.8204 X_1 = 0 \\ \frac{\partial Y}{\partial X_2} &= 2.0211 + 0.0044 X_1 - 0.0348X_3 - 0.0148 X_2 = 0 \\ \frac{\partial Y}{\partial X_3} &= 6.6017 + 0.0047X_1 - 0.0348 X_2 - 0.139X_3 = 0 \end{aligned}$$

**S 2**

$$\begin{aligned} \frac{\partial Y}{\partial X_1} &= 49.4083 + 0.0044 X_2 + 0.1488X_3 - 10.8204 X_1 = 0 \\ \frac{\partial Y}{\partial X_2} &= -0.5007 + 0.0044 X_1 + 0.0371X_3 - 0.0148 X_2 = 0 \\ \frac{\partial Y}{\partial X_3} &= 1.4263 + 0.1488 X_1 + 0.0371 X_2 - 0.1202 X_3 = 0 \end{aligned}$$

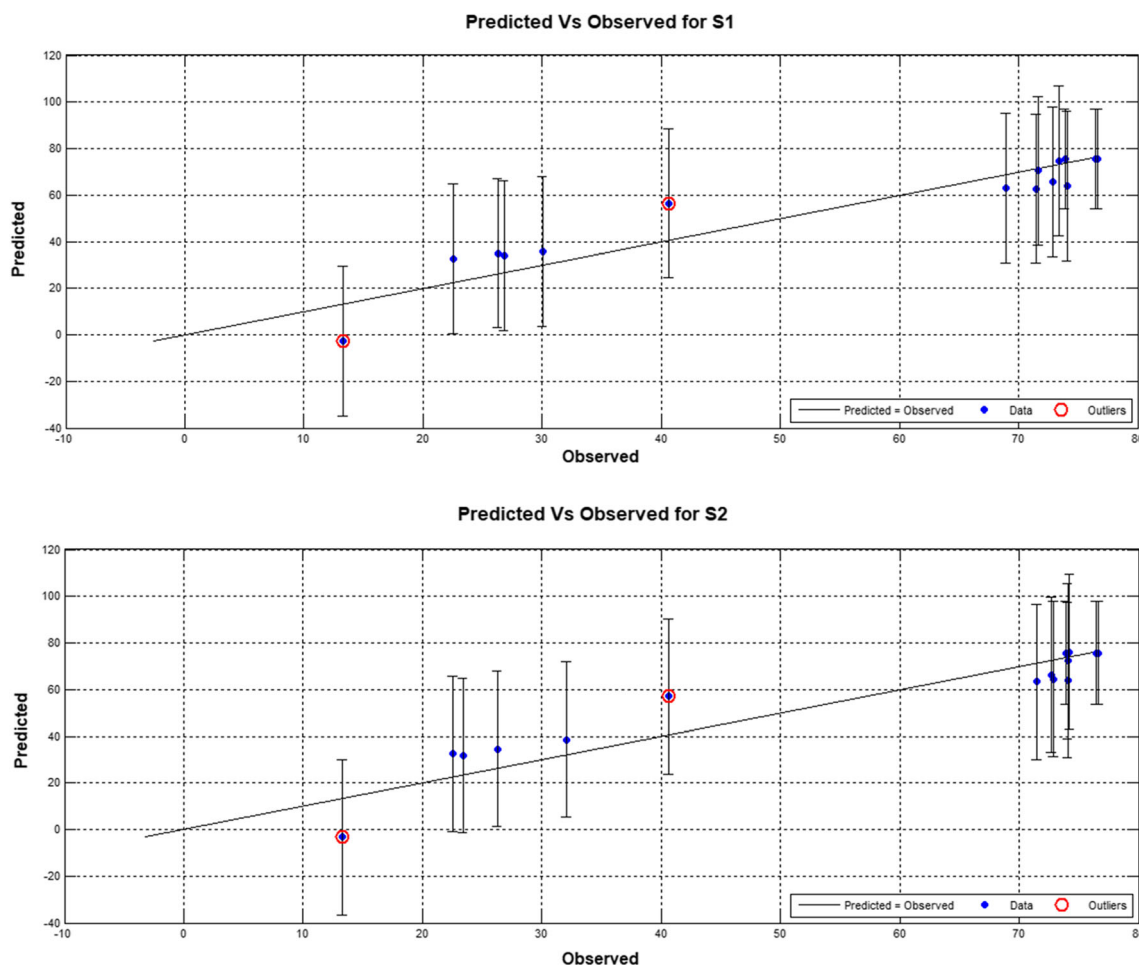


**Fig. 2** Parity plots showing the distribution of experimental vs. predicted values with the uncertainties of each fitted value of Ba<sup>2+</sup> percentage removal for S1 and S2

**Table 4** Regression coefficients estimated by multiple linear regression for S1 and S2

Terms	Coefficient	S1				S2			
		Value	Standard error of coefficient	<i>t</i> -value	<i>p</i> value	Value	Standard error of coefficient	<i>t</i> -value	<i>p</i> value
intercept	$\beta_0$	-227.9000	171.5900	-1.3282	0.2415	-56.6140	196.4800	-0.2880	0.7848
pH(L)	$\beta_1$	54.0000	24.4180	2.2387	0.9753	49.4080	27.9820	1.7657	0.1377
Time(L)	$\beta_2$	2.0211	1.4083	1.4562	0.2107	-0.5007	1.2820	-0.3884	0.7136
Temperature(L)	$\beta_3$	6.6017	6.7888	0.9724	0.3754	1.4265	7.0412	0.2025	0.8474
pH*Time	$\beta_{12}$	0.0044	0.1067	0.0414	0.9685	0.0044	0.1107	0.0399	0.9696
pH*Temperature	$\beta_{13}$	0.0047	0.5063	0.0093	0.9929	0.1488	0.5252	0.2834	0.7882
Time*Temperature	$\beta_{23}$	-0.0347	0.0292	-1.1901	0.2874	0.0370	0.0303	1.2225	0.2760
pH(Q)	$\beta_{11}$	-5.4102	1.4618	-3.7010	0.0139*	-5.4102	1.5161	-3.5684	0.0160*
Time(Q)	$\beta_{22}$	-0.0073	0.0048	-1.5089	0.1916	-0.0073	0.0051	-1.4549	0.2054
Temperature(Q)	$\beta_{33}$	-0.0694	0.0832	-0.8351	0.4416	-0.0601	0.0863	-0.6948	0.5171

\*Significant at  $p \leq 0.05$

The significance of each coefficient in the equations above is determined by Student’s *t* test and *p* value. Usually, coefficients with *p* value  $\leq 0.05$  represent the significant factors which directly affect the experimental procedure. As shown in Table 4, pH in its quadratic form is found to be a significant factor in the two systems (*p* value  $\leq 0.05$ ), while all other *p* values for other factors in their linear and interactions forms are above 0.05. This interpretation was explained via histograms presented in Fig. 3. Each histogram demonstrates the

interaction among two factors while the third is considered independent. The intercept of time and temperature is at 35 °C. This data gave an idea that the alteration of the pH affects directly the extraction of Ba<sup>2+</sup> from water samples so this factor should be taken into consideration as priority.

In addition, the results of the second order response surface model fitted in the form of ANOVA are presented in Table 5. It allows to determine the accuracy and adequacy of the two tested systems. The *F*-value (Fisher variance ratio) is a

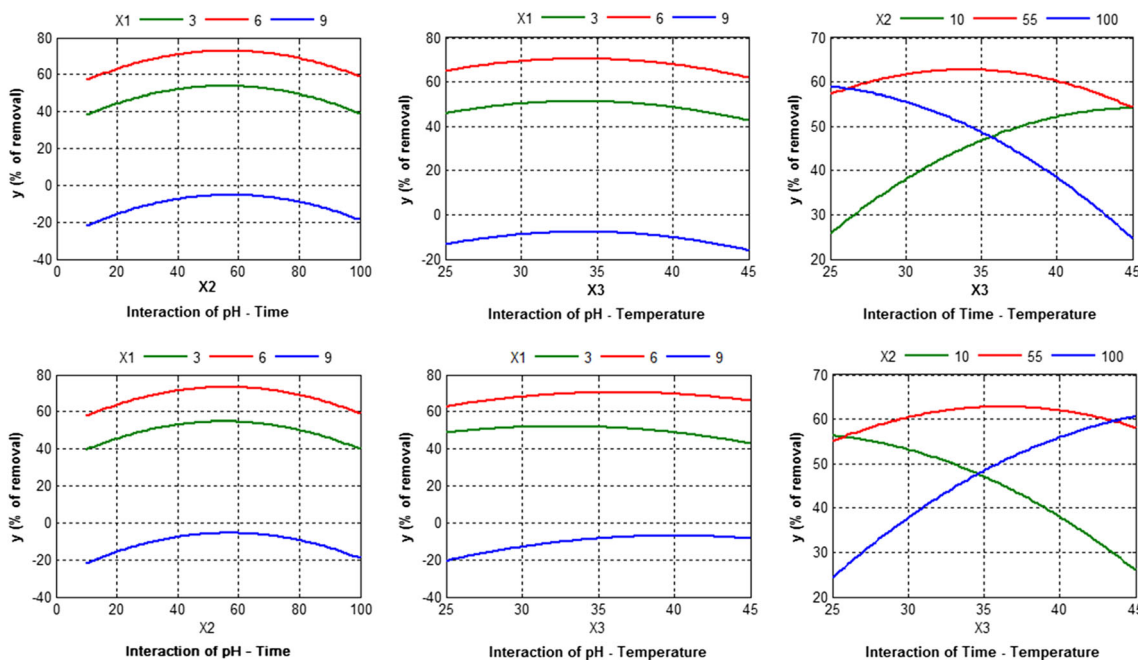


**Fig. 3** Graphs representing the interaction of the three factors (pH, time, and temperature), each two collectively, regarding their maximum, center, and minimum values for S1 (top) and S2 (bottom)

statistically valid measure of how well the factors describe the variation in the data about its mean. The greater the  $F$ -value is from unity, the more certain it is that the factors explain adequately the variation in the data about its mean, and the estimated factor effects are real (Karanam et al.). This analysis of the regression model demonstrates that the model is significant as evidenced by the  $F$ -values and the probability  $p$  values. As it can be seen in Table 5,  $F_{\text{model}}$  are equal to 3.8794 and 3.7387 for S1 and S2 respectively, and are associated with low probability values ( $P_{\text{model}} > F$ ) equal to 0.074796 for S1 and 0.080187 for S2. The adequacy and reliability of this study is presented by significant  $R$  and  $R^2$  values (Table 5). For S1 and S2,  $R$  is equal to 0.9349 and 0.9331 while  $R^2$  is equal to 0.87473 and 0.87063, respectively. The minor difference between  $R^2$  values of S1 and S2 could give the preference to the conditions presented in the first system and this is proved later by experiments.

In order to calculate the optimal pH, temperature, and contact time, the derivative matrix has been built and presented below. The optimal values  $X_{1s}$ ,  $X_{2s}$ , and  $X_{3s}$ , respectively, were calculated for the two systems, where for S1 the estimated value for the predicted extraction percentage was 80.46% at pH 5.1 during an agitation of 64.2 min at 31.6 °C for S1. As for S2, the percentage of removal is predicted to be 80.36% at pH 5.1 for an agitation of 59.4 min at 36.6 °C. The experimental percentage of  $\text{Ba}^{2+}$  removal from solution at the previously predicted optimums yielded 78.2% and 77.4% of extraction for systems 1 and 2, respectively. Experimental tests for S1 and S2 presented similar results in comparison with the maximal estimated extraction capacities at the optimal predicted values of pH, contact time, and temperature. As well, very close  $R^2$  values were obtained for both systems 1 and 2, so that it would be difficult to precise the preferred one immediately; this will be determined based on the presentation of interactions histograms.

### S1

$$X_s = \begin{vmatrix} X_{1s} \\ X_{2s} \\ X_{3s} \end{vmatrix} = \begin{vmatrix} -10.82038 & 0.00442422 & 0.00474017 \\ 0.00442422 & -0.01470526 & -0.0347933 \\ 0.00474017 & -0.0347933 & -0.138936 \end{vmatrix}^{-1} \begin{vmatrix} -54.6652 \\ -2.02110 \\ -6.60173 \end{vmatrix}$$

### S2

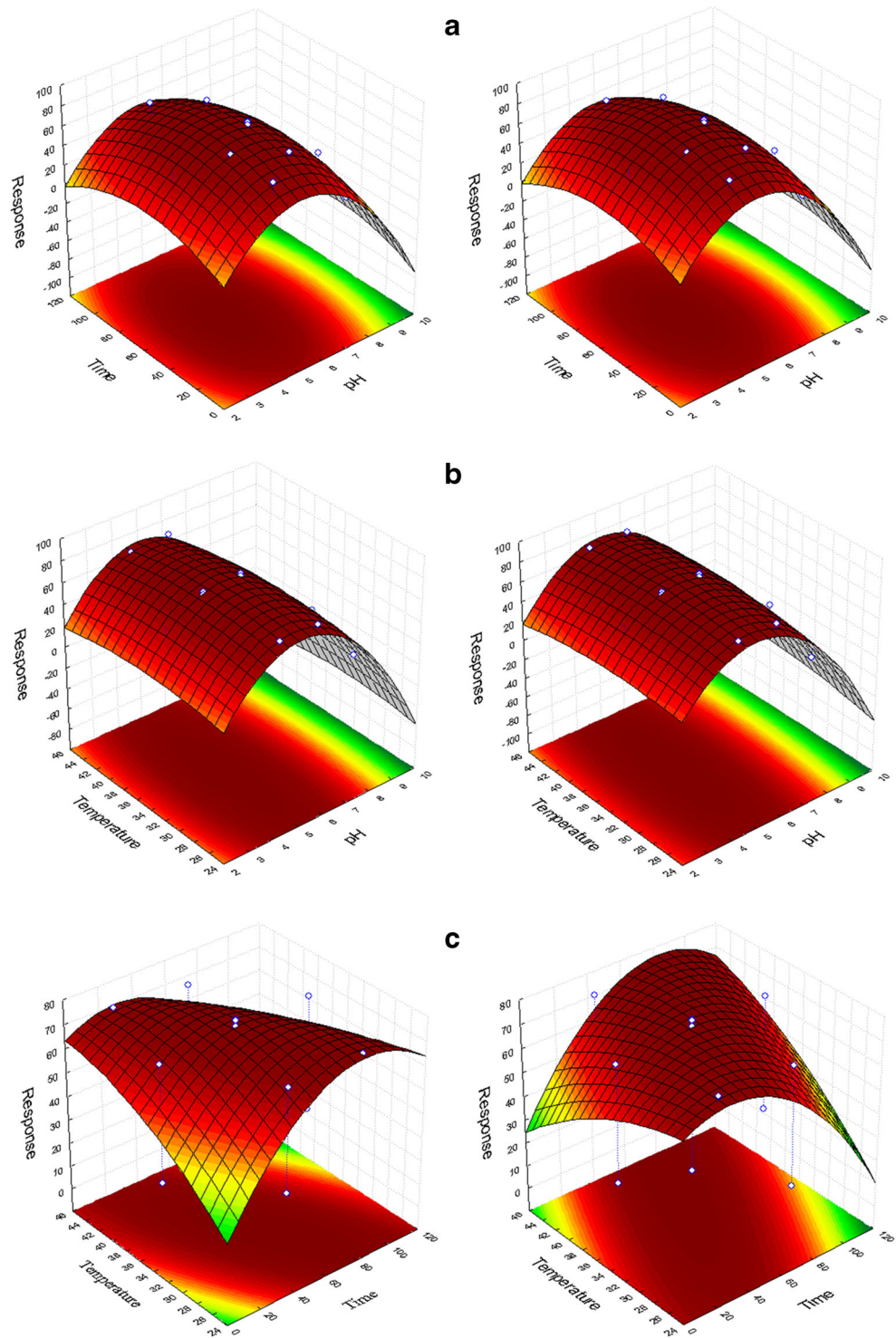
$$X_s = \begin{vmatrix} X_{1s} \\ X_{2s} \\ X_{3s} \end{vmatrix} = \begin{vmatrix} -10.82038 & 0.00442422 & 0.148834 \\ 0.00442422 & -0.01470526 & 0.0370686 \\ 0.148843 & 0.03470686 & -0.1202124 \end{vmatrix}^{-1} \begin{vmatrix} -49.4083 \\ 0.5007 \\ -1.4263 \end{vmatrix}$$

Eigenvalues of the matrix  $B/2$  are found to be  $-0.0028133$ ,  $-0.074028$ , and  $-5.4102$ , and  $-0.0013789$ ,  $-0.065044$ , and  $-5.4112$  for systems S1 and S2 respectively. These values lead to a percentage removal of  $\text{Ba}^{2+}$  with unique maximum. The response of surface plot for the interaction between the experimental factors is shown in Fig. 4a–c. Panel a presents the response of the surface plot of the interaction between pH vs. time with a temperature value fixed at 35 °C. The response increased with the rise of pH values in order to attend the maximum at a value around 5 for S1 and between 4.5 and 5 for S2. However, it decreased for the two systems when pHs are out of these intervals. The maximum time range was identified around 60 min and between 55 and 60 min for S1 and S2, respectively. The response variation during time range was minor. As presented in Fig. 4b, the response surface plot for the effect of pH vs. temperature was investigated with a time of contact fixed at 55 min. For the two systems, the instant increase of response with the rise of pH was observed while the trend is negligible for the temperature. The maximum values have been identified at pH 5 and between 33 and 36 °C for S1. For S2, the pH persists around 5 but the range of temperature increases to become between 32 and 37 °C. The histogram, presented in parts a and b from Fig. 3, explains the independence of

**Table 5** ANOVA for the entire quadratic model

Source	Some of squares (SS)	Degree of freedom (d.f.)	Mean squares (MS)	$F$ -value	probe> $F$
<b>S1</b>					
Error	1038.52175	5	207.7043	3.8794	0.074796
Model	7251.8753	9	805.7639		
Total	8290.397	14			
$R^2 = 0.87473$ , $R = 0.9349$					
<b>S2</b>					
Error	1117.1627	5	223.4325	3.7387	0.080187
Model	7518.0492	9	835.3388		
Total	8635.2119	14			
$R^2 = 0.87473$ , $R = 0.9349$					

**Fig. 4** Response surface and contour plot of **a** pH vs. time, **b** pH vs. temperature, and **c** time vs. temperature. (left side column is for S1 and right side column is for S2)

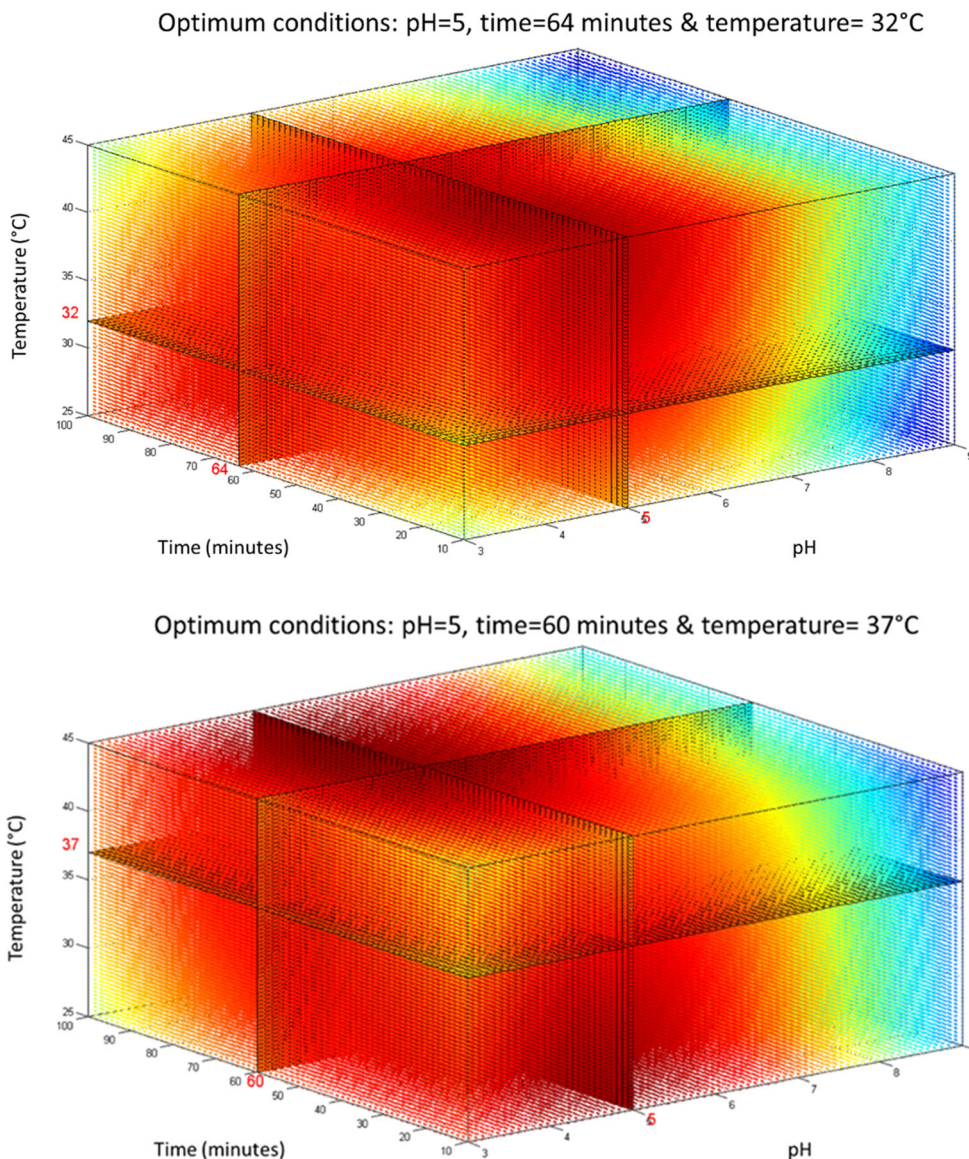


pH from other experimental parameters where it could affect alone the removal while the part c demonstrates the dependence of time and temperature for the removal of  $Ba^{2+}$  from water solutions. This dependency was demonstrated through the increase of response with the rise of values for the two factors for S1 to reach a maximum at around 60 min and 32 °C. This increase was followed by

a negligible decrease of response beyond these values. For S2, the optimal range is very broad; it is between 40 and 60 min in the time scale while the optimal temperature is higher than 46 °C. The last value of temperature is out of the experimental plan range.

These results lead to the conclusion that S1 is the more precise experimental plan presenting optimal conditions for

**Fig. 5** 3D presentations showing the interaction of the three factors (pH, time, and temperature) and the coordinates of the optimum value for each factor (marked in red) for S1 (top) and S2 (bottom)



removal of Ba<sup>2+</sup> from aqueous medium. Results of the 3D presentations, given in Fig. 5, show more clearly results obtained for the two systems, where strong interaction is depicted at the optimum values in S1 and a weak interaction at optimum values in S2.

**New approach for the calculation of optimal values by using direct equation**

In this study, a new calculation approach for the identification of optimal conditions has been demonstrated below. The details of the method for finding the equation have been presented in Sup 6.1.

$$X_i = \frac{(\beta_{jk}^2 - 4\beta_{jj}\beta_{kk})(2\beta_{jj}\beta_i - \beta_j\beta_{ji}) + (2\beta_{jj}\beta_k - \beta_{jk}\beta_j)(2\beta_{jj}\beta_{ik} - \beta_{jk}\beta_{ji})}{(\beta_{jk}^2 - 4\beta_{jj}\beta_{kk})(\beta_{ji}^2 - 4\beta_{jj}\beta_{ii}) - (2\beta_{jj}\beta_{ik} - \beta_{jk}\beta_{ji})(2\beta_{jj}\beta_{ik} - \beta_{jk}\beta_{ji})} \quad (6)$$

where  $i = \{1; 2; 3\}$ ;  $j = \{3; 1; 1\}$ ;  $k = \{2; 3; 2\}$  ( $ij = ji$ ,  $ik = ki$ ,  $jk = kj$ )

In order to simplify the equation, the values have been presented by:

$$A_i = \beta_{jk}^2 - 4\beta_{jj}\beta_{kk}, \quad A_j = \beta_{ji}^2 - 4\beta_{jj}\beta_{ii} \quad \& \quad A_k = 2\beta_{jj}\beta_{ki} - \beta_{ji}\beta_{jk}$$

$$X_i = \frac{\sum_{p=i \& p=k} (2\beta_{jj}\beta_p - \beta_j\beta_{jp}) * A_p}{A_i * A_j - A_k^2}$$

MATLAB program was used to obtain the optimal values of factor 1 as pH, 2 as time and 3 as temperature:

$$X_1 = \frac{(\beta_{23}^2 - 4\beta_{33}\beta_{22})(2\beta_{33}\beta_1 - \beta_3\beta_{13}) + (2\beta_{33}\beta_2 - \beta_{23}\beta_3)(2\beta_{33}\beta_{12} - \beta_{23}\beta_{13})}{(\beta_{13}^2 - 4\beta_{33}\beta_{22})(\beta_{13}^2 - 4\beta_{33}\beta_{11}) - (2\beta_{33}\beta_{12} - \beta_{23}\beta_{13})(2\beta_{33}\beta_{12} - \beta_{23}\beta_{13})}$$

$$X_2 = \frac{(\beta_{13}^2 - 4\beta_{33}\beta_{11})(2\beta_{11}\beta_2 - \beta_1\beta_{12}) + (2\beta_{11}\beta_3 - \beta_{13}\beta_1)(2\beta_{11}\beta_{23} - \beta_{13}\beta_{12})}{(\beta_{13}^2 - 4\beta_{33}\beta_{11})(\beta_{12}^2 - 4\beta_{22}\beta_{11}) - (2\beta_{11}\beta_{23} - \beta_{13}\beta_{12})(2\beta_{11}\beta_{23} - \beta_{13}\beta_{12})}$$

$$X_3 = \frac{(\beta_{12}^2 - 4\beta_{22}\beta_{11})(2\beta_{11}\beta_3 - \beta_1\beta_{13}) + (2\beta_{11}\beta_2 - \beta_1\beta_{12})(2\beta_{11}\beta_{23} - \beta_{13}\beta_{12})}{(\beta_{12}^2 - 4\beta_{22}\beta_{11})(\beta_{13}^2 - 4\beta_{33}\beta_{11}) - (2\beta_{11}\beta_{23} - \beta_{13}\beta_{12})(2\beta_{11}\beta_{23} - \beta_{13}\beta_{12})}$$

Results of Eq. 6 were identical to the ones obtained previously by the matrix calculations with optimal values equal to pH 5.09, 64.2 min, and 31.6 °C. These results showed that this equation could be engaged in order to facilitate the identification of optimal conditions by using simpler approaches for calculations.

## Conclusion

The present study involved the Doehlert experimental plan in the identification of optimal conditions for the removal of Ba<sup>2+</sup> from aqueous media by a new polymer material (CPP) based on phenoxycalix[4]pyrrole. Barium was used as a model compound to avoid radioactive waste since it has a chemical behavior similar to Ra-226. The effect of the amount of CPP has been studied, and 75 mg was identified as the optimal mass. The pH, the contact time, and the temperature were selected as experimental factors that could affect the percentage removal of cations from aqueous media. These factors were optimized through a Doehlert experimental plan using MATLAB (regstat) and STATISTICA 7 for the necessary computation. Optimal values were determined to be pH = 5, contact time = 64 min, and temperature = 31.6 °C for the solution during extraction and lead to a Ba<sup>2+</sup> extraction yield of 78.2%. These results have been presented by different 2D and 3D histograms. Referring to these histograms, pH has been identified as a significant factor and independent from the other factors, while time and temperature are dependent. At the end and in order to facilitate the calculation of the optimal conditions, a new approach has been developed, tested, and presented by Eq. 6. Same results were obtained by using the new equation and the matrix. This study was the first using Doehlert experimental plan to optimize the removal of cations from water, using an upgraded phenoxycalix[4]pyrrole compound. It could open the door to other experimental strategies that could be engaged for the optimization of experimental parameters for the removal of materials (organic or inorganic) from aqueous media. These experimental conditions will be applied to test the removal of Ra-226 from solutions and results will be reported in due course.

## Acknowledgments

The authors would like to thank the Lebanese National Council for Scientific Research (CNRS-L) for GRP fund support and AUF/CNRS–SCORE project.

## References

- Abbas I, Hannud H, Shamsaldeen HC (2012) Calix[4]pyrrole macrocycle: extraction of fluoride anions from aqueous media. *Chem Eur J* 3(2):156–162. <https://doi.org/10.5155/eurjchem.3.2.156-162.542>
- Abbas II, Chaaban JK (2012) Pyridine-substituted calix[4]pyrrole: a new cation receptor. *Supramol Chem* 24(3):213–219. <https://doi.org/10.1080/10610278.2011.643795>
- AlHaddad N, Rifai A, Kasprowiak A, Cazier-Dennin F, Danjou P-E (2019) Solid–liquid extraction of iodide and bromide from aqueous media by a new water-insoluble phenoxycalix[4]pyrrole-epichlorohydrin polymer. *Org Biomol Chem* 17:7330–7336. <https://doi.org/10.1039/C9OB01306G>
- Anzenbacher P, Jursíková K, Lynch VM, Gale PH, Sessler JL (1999) Calix[4]pyrroles containing deep cavities and fixed walls. Synthesis, structural studies, and anion binding properties of the isomeric products derived from the condensation of p-Hydroxyacetophenone and Pyrrole. *J Am Chem Soc* 121:11020–11021. <https://doi.org/10.1021/ja993195n>
- Bassioni G, Abdulla F, Morsy Z, El-Faramawy N (2012) Evaluation of naturally occurring radioactive materials (norms) in inorganic and organic oilfield scales from the middle east. *Arch Environ Contam Toxicol* 62(3):361–368. <https://doi.org/10.1007/s00244-011-9706-7>
- Bonomo L, Solari E, Toraman G, Scopelliti R, Latronico M, Floriani C (1999) A cylindrical cavity with two different hydrogen-binding boundaries: the calix[4]arene skeleton screwed onto the meso-positions of the calix[4]pyrrole. *Chem Commun* (23):2413–2414. <https://doi.org/10.1039/A907563A>
- Camiolo S, Gale PA (2000) Fluoride recognition in ‘super-extended cavity’ calix[4]pyrroles. *Chem Commun*:1129–1130. <https://doi.org/10.1039/B003229H>
- Chen X, Ji M, Fisher DR, Wai CM (1999) Ionizable calixarene-crown ethers with high selectivity for radium over light alkaline earth metal ions. *Inorg Chem* 38(23):5449–5452. <https://doi.org/10.1021/ic990135+>
- Chiarizia R, Dietz ML, Horwitz EP, Burnett WC, Cable PH (1999) Radium separation through complexation by aqueous crown ethers and ion exchange or solvent extraction. *Sep Sci Technol* 34(6–7):931–950. <https://doi.org/10.1080/01496399908951074>
- Chi X, Peters GM, Hammel F, Brockman C, Sessler JL (2017) Molecular recognition under interfacial conditions: calix[4]pyrrole-based cross-linkable micelles for ion pair extraction. *J Am Chem Soc* 139(27):9124–9127. <https://doi.org/10.1021/jacs.7b04529>
- Danil de Namor A, Shehab M, Khalife R, Abbas I (2007b) Modified calix[4]pyrrole receptor: solution thermodynamics of anion complexation and a preliminary account on the phosphate extraction ability of its oligomer. *J Phys Chem B* 111(42):12177–12184. <https://doi.org/10.1021/jp073863o>
- Danil de Namor AF, Abbas I, Hammud HH (2007a) A new calix[4]pyrrole derivative and its anion (fluoride)/Cation (mercury and silver) recognition. *J Phys Chem B* 111(12):3098–3105. <https://doi.org/10.1021/jp067798e>

- Dani de Namor AF, Khalife R (2008) Calix[4]Pyrrole derivative: recognition of fluoride and mercury ions and extracting properties of the receptor-based new material. *J Phys Chem B* 112(49):15766–15774. <https://doi.org/10.1021/jp8045356>
- Doehlert DH (1970) Uniform Shell designs. *J Royal Stat Soc* 19(3):231–239. <https://doi.org/10.2307/2346327>
- Dutra RL, Maltez HF, Carasek E (2006) Development of an on-line preconcentration system for zinc determination in biological samples. *Talanta* 69(2):488–449. <https://doi.org/10.1016/j.talanta.2005.10.019>
- Eisenbud M, Gesell TF (4<sup>th</sup> ed) (1997) Environmental radioactivity from natural, industrial & military sources. Elsevier, San Diego, Academic press
- Fard AK, Rhadfi T, Khraisheh M, Atieh MA, Khraisheh M, Hilal N (2016) Reducing flux decline and fouling of direct contact membrane distillation by utilizing thermal brine from MSF desalination plant. *Desalination* 379:172–181. <https://doi.org/10.1016/j.desal.2015.11.004>
- Ferreira SLC, Santos WNL, Quintella CM, Net BB, Bosque-Sendra JM (2004) Doehlert matrix: a chemometric tool for analytical chemistry—review. *Talanta* 63(4):1061–1067. <https://doi.org/10.1016/j.talanta.2004.01.015>
- Gott M, Yang P, Kortz U, Stephan H, Pietzsch HJ, Mamat C (2019) A <sup>224</sup>Ra-labeled polyoxopalladate as putative radiopharmaceutical. *Chem Commun*. <https://doi.org/10.1039/C9CC02587A>
- Henriksena G, Hoffa P, Larsena RH (2002) Evaluation of potential chelating agents for radium. *Appl Radiat Isot* 56(5):667–671. [https://doi.org/10.1016/S0969-8043\(01\)00282-2](https://doi.org/10.1016/S0969-8043(01)00282-2)
- Imandi SB, Bandaru VVR, Somalanka SR, Garapati HR (2007) Optimization of medium constituents for the production of citric acid from byproduct glycerol using Doehlert experimental design. *Enzym Microb Technol* 40(5):1367–1372. <https://doi.org/10.1016/j.enzmictec.2006.10.012>
- Karanam SK, Medicherla NR (2010) Application of Doehlert experimental design for the optimization of medium constituents for the production of L asparaginase from palm Kernel cake (*Elaeis guineensis*). *J Microbial Biochem Technol* 2(1):1–7. <https://doi.org/10.4172/1948-5948.1000016>
- Kondash AJ, Warner NR, Lahav O, Vengosh A (2013) Radium and barium removal through blending hydraulic fracturing fluids with acid mine drainage. *Environ Sci Technol* 48(2):1334–1342. <https://doi.org/10.1021/es403852h>
- Matyskin AV, Brown PL, Ekberg C (2019) Weak barium and radium hydrolysis using an ion exchange method and its uncertainty assessment. *J Chem Thermodynamics* 128:362–371. <https://doi.org/10.1016/j.jct.2018.08.037>
- Majeed FA, Abojassim AA, Mesehour Ali A (2019) Radiological risk due to NORM in soil samples at Al-Samawah desert of Al-Muthanna governorate, Iraq. *Iranian J Med Phys* 0(0). <https://doi.org/10.1016/j.jct.2018.08.037>
- McDevitt B, McLaughlin M, Cravotta CA, Ajemigbitse MA, Van Sice KJ, Blotevogel J, Borch T, Warner NR (2018) Emerging investigator series: radium accumulation in carbonate river sediments at oil and gas produced water discharges: implications for beneficial use as disposal management, *environ. Sci. Processes Impacts* 21(2):324–338. <https://doi.org/10.1039/C8EM00336J>
- McDowell WJ, Case GN, Bartsch RA, Czech BP (1986) Solvent extraction of radium and barium cations into chloroform by a lipophilic acyclic polyether dicarboxylic acid. *Solvent Extr Ion Exch* 4(3):411–419. <https://doi.org/10.1080/07366298608917874>
- Mishra SP, Tiwary D (1999) Ion exchangers in radioactive waste management. Part XI Removal of barium and strontium ions from aqueous solutions by hydrous ferric oxide. *Appl Radiat Isot* 51(4):359–366. [https://doi.org/10.1016/S0969-8043\(99\)00065-2](https://doi.org/10.1016/S0969-8043(99)00065-2)
- Mokhodoeva O, Vlk M, Ma'lkova' E, Kukleva E, Mic'olova' P, S'tamberg K, S'louf M, Dzhenloda R, Kozempel J (2016) Study of <sup>223</sup>Ra uptake mechanism by Fe<sub>3</sub>O<sub>4</sub> nanoparticles: towards new prospective theranostic SPIONs. *J Nanopart Res* 18:301–312. <https://doi.org/10.1007/s11051-016-3615-7>
- Nafae TM, Ahmedzeki NS, Zayir YM, Zaidan W, El Samad O, Bou Khozam R (2016) Chemical treatment of contaminated soil with naturally occurring radioactive materials “NORM” by leaching with different solvents. Thirteenth Arab conference on the peaceful uses of atomic energy. Republic of Tunisia, Hammamet
- Reissig F, Bauer D, Pietzsch HJ, Steinbach J, Mamat C (2019) Synthesis and functionalization of radium-doped barium sulfate nanoparticles. *J Med Imaging Radiat Sci* 50:S38. <https://doi.org/10.1016/j.jmir.2019.03.117>
- Rifai A, AlHaddad N, Noun M, Abbas I, Tabbal M, Shatila R, Cazier-Dennin F, Danjou PE (2019) A click mediated route to a novel fluorescent pyridino-extended calix[4]pyrrole sensor: synthesis and binding studies. *Org Biomol Chem* 17(23):5818–5825. <https://doi.org/10.1039/C9OB01106D>
- Sharma S, Kumar A, Mehra R, Mishra R (2019) Radiation hazards associated with radionuclides and theoretical evaluation of indoor radon concentration from soil exhalation of Udhampur District, Jammu and Kashmir state, India. *J Soils Sediments* 19(3):1441–1455. <https://doi.org/10.1007/s11368-018-2125-x>
- Silas S, Sailaja D, Rao GH (2016) Doehlert 4-variable design for the optimization of lead biosorption using activated carbon derived from palm kernel cake. *IJRSET* 5(4):5225–5236. <https://doi.org/10.15680/IJRSET.2016.0504127>
- Vanot G, Valérie D, Guilhem MC, Phan-Tan-Luu R, Comeau LC (2002) Maximizing production of Penicillium cyclopium partial acylglycerol lipase. *Appl Microbial Biotechnol* 60(4):417–419. <https://doi.org/10.1007/s00253-002-1144-z>
- Vengosh A, Hirschfeld D, Vinson D, Dwyer G, Raanan H, Rimawi O, Al-Zoubi A, Akkawi E, Marie A, Haquin G, Zaarur S, Ganor J (2009) High naturally occurring radioactivity in fossil groundwater from the middle east. *Environ Sci Technol* 43(6):1769–1775. <https://doi.org/10.1021/es802969r>
- Ward Whicker F (1997) Environmental radioactivity from natural, industrial, and military sources. Merrill Eisenbud, Thomas Gesell. *Radiat Res* 148(4):402–403. <https://doi.org/10.2307/3579528>
- Yang D, Xu B, Burnett W, Yu Z, Jiang X, Zhang X, Zhao S, Xia D (2018) Radium isotopes—suspended sediment relationships in a muddy river. *Chemosphere* 214:250–258. <https://doi.org/10.1016/j.chemosphere.2018.09.058>
- Zayir YM, Ahmedzeki NS, El Samad O, Nafae TM, Zaidan W, Bou Khozam R (2016) Radiological assessment and mechanical separation of norm contaminated soil from iraqi oil fields. *IJCPE* 17(2):25–35
- Zhang T, Gregory K, Hammack RW, Vidic RD (2014) Co-precipitation of radium with barium and strontium sulfate and its impact on the fate of radium during treatment of produced water from unconventional gas extraction. *Environ Sci Technol* 48(8):4596–4603. <https://doi.org/10.1021/es405168b>
- Zielinski RA, Al-Hwaiti MS, Budahn JR, Ranville JF (2011) Radionuclides, trace elements, and radium residence in phosphogypsum of Jordan. *Environ Geochem Health* 33(2):149–165. <https://doi.org/10.1007/s10653-010-9328-4>

**Publisher's note** Springer Nature remains neutral with regard to jurisdictional claims in published maps and institutional affiliations.